Journal of Innovations in Computer Science and Engineering
Shahid Beheshti Unversity

June 2024, Special Issue on AI 4 All- 1

Application of machine learning algorithms in the prediction of the reliability of post-tensioned concrete members

Pooria Poorahad A, ORCID ID: 0000-0002-7173-9975
Faculty of Civil, Water, and Environmental Engineering, Shahid Beheshti University, Tehran, Iran, p_poorahadanzabi@sbu.ac.ir
Mahmoud R. Shiravand, ✉, ORCID ID: 0000-0002-8740-2242
Faculty of Civil, Water, and Environmental Engineering, Shahid Beheshti University, Tehran, Iran, m_shiravand@sbu.ac.ir
Mahtab Ebadati,
Faculty of Civil, Water, and Environmental Engineering, Shahid Beheshti , University Tehran, Iran, m.ebadati@mail.sbu.ac.ir

Abstract—Structural reliability analysis (SRA) is associated with complex calculations and large number of simulations. In this paper, machine learning (ML) methods are integrated with SRA to reduce the overall intricacy and computational cost of direct SRA methods, such as the Monte Carlo simulation (MCS) method. An SRA is conducted in this paper on post-tensioned concrete members under the influence of prestress loss, and their reliability indices are obtained through the MCS method. The results of the SRA are used to create a database for data fitting of the ML algorithms. The algorithms are compared to find the most accurate ML model to be applied on the problem at hand. For the SRA, different stochastic parameters with specified probabilistic distributions are considered for the numerical models, and nonlinear dynamic analyses are conducted on them. Using the labeled data resulted from the SRA, five ML algorithms are compared; (i) linear regression, (ii) random forest, (iii) artificial neural network, (iv) k-nearest neighbors, (v) extreme gradient boosting. R-squared and root mean squared error are considered as the metrics used for the comparison of the ML models. Bayesian search is used for hyperparameter optimization of algorithms. The performance of the linear regression algorithm (R2 = 0.67 and RMSE = 0.26)
indicates that the SRA problems are highly nonlinear and linear algorithms cannot precisely map the relationships in data. However, the results show that extreme gradient boosting has the finest accuracy with R2 = 0.9 and RMSE = 0.04. Additionally, its predicted values mostly have relative errors of less than ±30%. The closeness of performances of testing and training sets indicates that overfitting is avoided for all 5 predictive models.

Keywords—artificial intelligence, machine learning, supervised learning, structural reliability analysis

I. Introduction

Machine learning (ML) is the specific area of artificial intelligence that allows computers to learn from data solving a given task [1]. ML methods are the product of the adoption of statistical theories in computational algorithms to predict or recognize patterns in data. Based on the availability of the sample data, the ML methods can be categorized into different types of algorithms: supervised, unsupervised, semi-supervised, active, and reinforcement learning algorithms [2]. Supervised
learning algorithms are used when the sample data contain input-output pairs, called labelled data, obtained from the desired function or distribution.

Recently, the application of supervised ML techniques has gained tremendous attention in the field of structural and earthquake engineering. This is due to the ability of ML-based models to predict the relationship between the predictors and response variable(s) without the need for the knowledge of underlying physical and mathematical models [3]. Given a well-developed analytical and numerical method for structural reliability analysis (SRA), such as First/Second-Order Reliability Methods (FORM/SORM), First Order Second Moment (FOSM), and Monte Carlo Simulation (MCS), the ML methods are appliable to engineering problems, and can outperform statistical and research-intensive efforts in a small fraction of the computational expense [4].

ML methods are widely applied to SRA problems related to bridges [5, 6]. Due to the importance of bridges in lifeline systems, self-centering post-tensioned (SCPT) piers are proposed to enhance the post-earthquake performance of bridges [7]. Post-tensioned (PT) tendons are used in SCPT piers to provide rocking stiffness and additional self-centering force but due to the prestress loss, the PT tendon loses some extent of its initial prestressing [8]. ML methods have been applied to SCPT piers [9, 10] but a comprehensive study is required to investigate the effect of prestress loss on reliability of SCPT piers.

With the development of computer science and artificial intelligence, useful methods are now provided to allow for assessment of bridges without the drawbacks and limitations of the experimental and numerical methods, and without any knowledge on the physical characteristics of the structure. With time, PT members cannot fulfill the performance objectives that they were initially designed for due to the loss of prestressing force. In this study, the application of ML models on prediction of reliability index

Submit Date: 2024-10-11
Accept Date: 2025-04-12
✉ Corresponding author

of SCPT piers is investigated. The prestress loss of PT tendons is essentially important in these structures due to their dependency on PT tendons to provide stiffness and limit residual drifts. As for it, five ML algorithms; (i) linear regression (LR), (ii) random forest (RF), (iii) artificial neural network (ANN), (iv) k-nearest neighbors (KNN), and (v) extreme gradient boosting (XGB) are employed to build predictive models. The database required for the data fitting of the models is created by finite element method (FEM). Bayesian search is considered for optimization of the hyperparameters of algorithms. R-squared and root mean squared error (RMSE) metrics are used for the comparison of the predictive models. The predictive models are compared with each other to find the most accurate one in prediction of reliability index of SCPT piers.

II. Methodology

Supervised learning is used when the labeled data is available. In this study, the labelled data are readily achievable through numerical analysis provided by FEM. Therefore, the supervised algorithms are the most applicable approach and the ML algorithms chosen for this study are in the supervised learning class. Fig. 1 shows the overall schematic process of supervised learning. In this figure, ψ is the unknown function or distribution to be modelled. The vector of inputs (features vector) is denoted by $\mathbf{x} \in \mathbb{R}^n$ where n is the number of features, and $\mathbf{y}$ is the output vector to be approximated. The set of input-output pairs, denoted by S, is obtained from the probability distribution of input space, $f_x(x)$. The subscript *i* refers to the ith sample data pair. The hypothesis space, H, is the set of all possible models, $h \in H$, to be selected by the learning algorithm. A hypothesis is defined by a set of parameters denoted by $\mathbf{w}$. The learning algorithm uses an optimization method to choose the optimum values of $\mathbf{w}$ regarding a defined cost function, such as Square Error and maximum likelihood. This optimization process is called *training of the model*. The estimation of ψ at each desired new operating point, $\mathbf{x}$, is the output of the trained model shown by $\hat{y}$.

In practice, the selection of hypothesis space, cost function and the optimization algorithm for selecting the model parameters depend on different factors, such as the number of features in the input vector, the size of the data pool, and the possible prior knowledge about the input and output data distribution. For example, the computational cost for some learning algorithms remarkably increases with the number of features. On the other hand, the application of some methods, such as Bayesian Regression for problems with a low number of features or highly correlated features, may result in high prediction errors.

Data collection is one of the main challenges in implementing artificial intelligence processes, due to the lack of relevant, accurate, and high-quality data. In the present research, the labeled data required for the database is created through a randomized experiment with stochastic parameters tabulated in Table 1 through FEM. This way of data creation is computationally extensive and time-consuming. However, the result is a well-structured and accurate database that leads to high-performance predictive models. Thus, numerical models of SCPT piers are built in the OpenSees [11] framework and the prestress loss is accounted for by calculating the losses from different sources [12, 13]. Six sources of prestress loss are considered in this study; (i) friction, (ii) anchorage set, (iii) elastic shortening, (iv) concrete creep, (v) concrete shrinkage, and (vi) steel relaxation. Friction, anchorage set, and elastic shortening are instantaneous while the others are time-dependent.

The numerical models are run, and the maximum drift, δ_{max}, and residual drift, δ_{res}, values are stored. To calculate the reliability of SCPT piers, it is required to define a state of failure and determine the probability of violating it. In structural reliability analysis problems, failure is defined using the concept of *performance state*. Two performance states can be considered for SCPT piers; (i) seismic performance and (ii) post-earthquake performance. Performance states are represented by performance functions as

$$g_{SP} = (\delta_{all})_{SP} - \delta_{\max} \quad (1)$$

$$g_{PP} = (\delta_{all})_{PP} - \delta_{res} \quad (2)$$

where g_{sp} and g_{pp} are the performance functions for seismic and post-earthquake performance states, respectively, $(\delta_{all})_{SP}$ and $(\delta_{all})_{SP}$ are corresponding allowable drifts. The allowable drifts for seismic and post-earthquake performances are adopted from antecedent studies [14, 15] and are tabulated in Table 2. The probability of failure, P_f, is expressed as:

TABLE I. STOCHASTIC PARAMETERS

Parameter	Distribution	Mean	COV
Concrete compressive strength (f_c)	Lognormal	32.5 MPa	20%
Nominal post-tensioning ratio (ρ_t)	Normal	0.4	10%
Relative annual humidity (H)	Normal	50%	15%
Superstructure weight (W)	Lognormal	1456 kN	25%
Ground motion record (EQ)	Uniform	50.5	56.6%

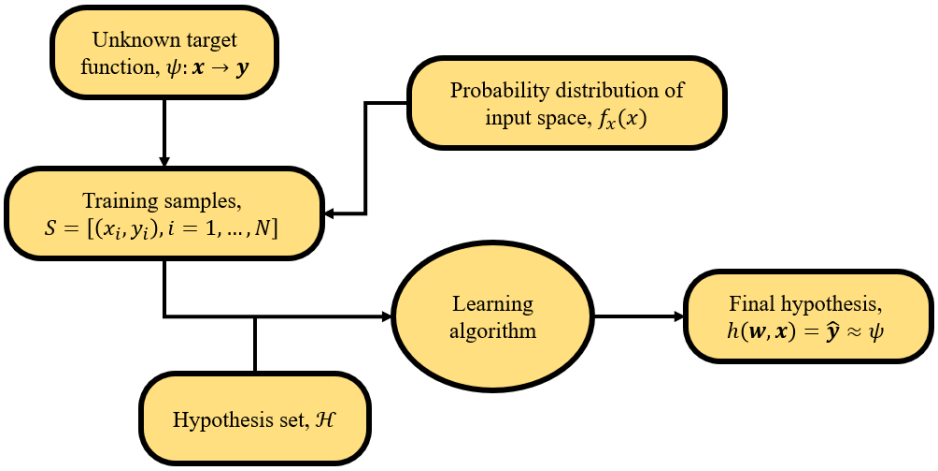

Fig. 1. Schematic procedure of supervised learning (adpted from [16]).

TABLE II. ALLOWABLE DRIFTS

Performance	Seismic level	Allowable drift	Performance Level
Seismic	DBE	2.0%	Serviceability
	MCE	4.5%	Collapse prevention
Post-earthquake	DBE	1/300	Emergent usage
	MCE	1/100	Reconstruction

$$P_f = P[g(x) \le 0] = \int f_x(x)dx \qquad (3)$$

where g(x) is the defined performance function and $f_x(x)$ is the joint probability density function of the vector of the basic random variable x. Direct evaluation of (3) is burdensome in general. Consequently, the MCS method is employed in this study to obtain the failure probability. The reliability of a structure is typically assessed by a single numeric indicator called the reliability index, β. The reliability index is mathematically defined as.

$$\beta = -\Phi^{-1}(P_f) \qquad (4)$$

where $\Phi^{-1}()$ is the inverse of the cumulative distribution function.

In addition to the parameters tabulated in Table 1, numerical models of SCPT piers are built in different aspect ratios (H/B = 3 ~ 10) and energy dissipation bar ratios (ρ_s = 0.0 ~ 1.0%) where $\rho_s = A_s/A_c$ is the ratio of energy dissipation bar cross-section area, A_s, to column cross-section area, A_c. The criterion for the selection of these parameters is to improve the generality of the study and account for different design conditions. The ground motion records with which the piers are excited are also randomly chosen from the ground motion records introduced in FEMA P695 [17]. All the ground motion sets including far-field and near-field records are chosen, constituting 100 ground motion records. The ground motion records are scaled to design-based earthquake (DBE) and maximum credible earthquake (MCE) spectra according to provisions of ASCE/SEI 7-16 [18]. The prestress loss is taken into account by a time-step method. In this method, the service life of a bridge is divided into a number of intervals, e.g. 10 in this study. Therefore, time is another input feature.

Fig. 2 shows the workflow of the present study. These parameters are considered as the labels of the input and the reliability index is considered as the label of the target parameter as tabulated in Table 3. At each time-step, the FEM analysis is iterated 400 times (at each iteration a random set of stochastic parameters is generated) and the labels of each analysis are stored to create the labelled data of the database. Collectively, 4000 FEM analyses are performed and thus, the database used in this study constitutes 4000 input-output pairs. Fig. 3 shows the frequency histograms of features provided by the randomized experiment from FEM. The entire database is randomly divided into a training set (80%) and a testing set (20%). One-hot encoding technique is used to convert categorial variables to numeric values by creating a binary column for each category, indicating that whether the category is present or not.

The ML algorithms are trained by the training set. Then, the features of the testing set are given to the predictive models and the prediction results are compared with the observed ones to assess the accuracy of the predictive models. Additionally, there exist a number of metrics to evaluate the accuracy of predictive models. R-squared, mean absolute error, mean squared error, and RMSE are the most commonly used metrics. Mean absolute error is the most straightforward metric. However, it is not affected by extreme errors. The mean squared error gives more weight to larger errors and thus it is penalized by large errors. The main disadvantage of this metric is that its unit is different from the target. Using RMSE, this drawback is overcome while still maintaining the sensitivity to the large errors. Accordingly, the R-squared and RMSE metrics are chosen in this paper to evaluate the performances of predictive models.

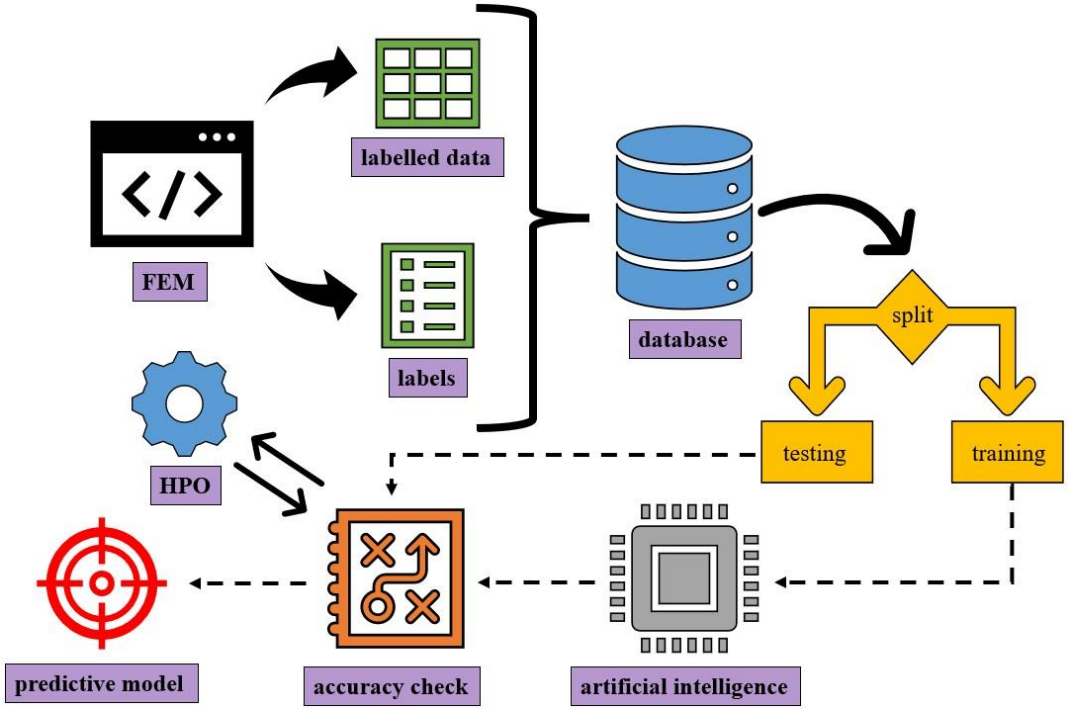

Fig. 2. Workflow of the present study.

TABLE III. LABELLED DATA OF THE DATABASE

Label	Parameter	Type	Class
f_c	Concrete compressive strength	Numerical	Feature
ρ_t	Nominal post-tensioning ratio	Numerical	Feature
H	Relative annual humidity	Numerical	Feature
W	Superstructure weight	Numerical	Feature
EQ	Ground motion record	Numerical	Feature
H/B	Aspect ratio	Numerical	Feature
ρ_s	Energy dissipation bar ratio	Numerical	Feature
T	Time	Numerical	Feature
SL	Seismic level	Categorial	Feature
PS	Performance state	Categorial	Feature
β	Reliability index	Numerical	Target

Every algorithm comes with additional hyperparameters that need to be configured to avoid problems such as overfitting, underfitting, convergence, etc. Hyperparameter optimization (HPO) algorithms are proposed to tackle these problems. The goal is to find $x^* \in \arg\min_{x \in X} f(x)$ in which $f : X \to$ □ is the function that maps from the hyperparameter space $x \in X$, and x^* is the set of hyperparameters with the best performance.. The most commonly used HPO algorithms are grid search, randomized search, and Bayesian search. Grid search investigates every possible combination of hyperparameters while randomized search tests a random combination of hyperparameters, and thus it is less time-consuming. However, these two algorithms do not consider the past results. Bayesian search improves the performance of the optimization by considering the previously selected hyperparameters when determining the next set. Hence, Bayesian search is utilized in this study. Using the Bayesian search algorithm, the best performance of the predictive models is yielded.

III. Machine Learning

As described in Sec. 2, after data fitting of the ML models, the features of the testing set are given to the predictive models, and the predictions are compared with the target of the data set (observed data) in Fig. 4. The same is done for the training data set so that the predictive model

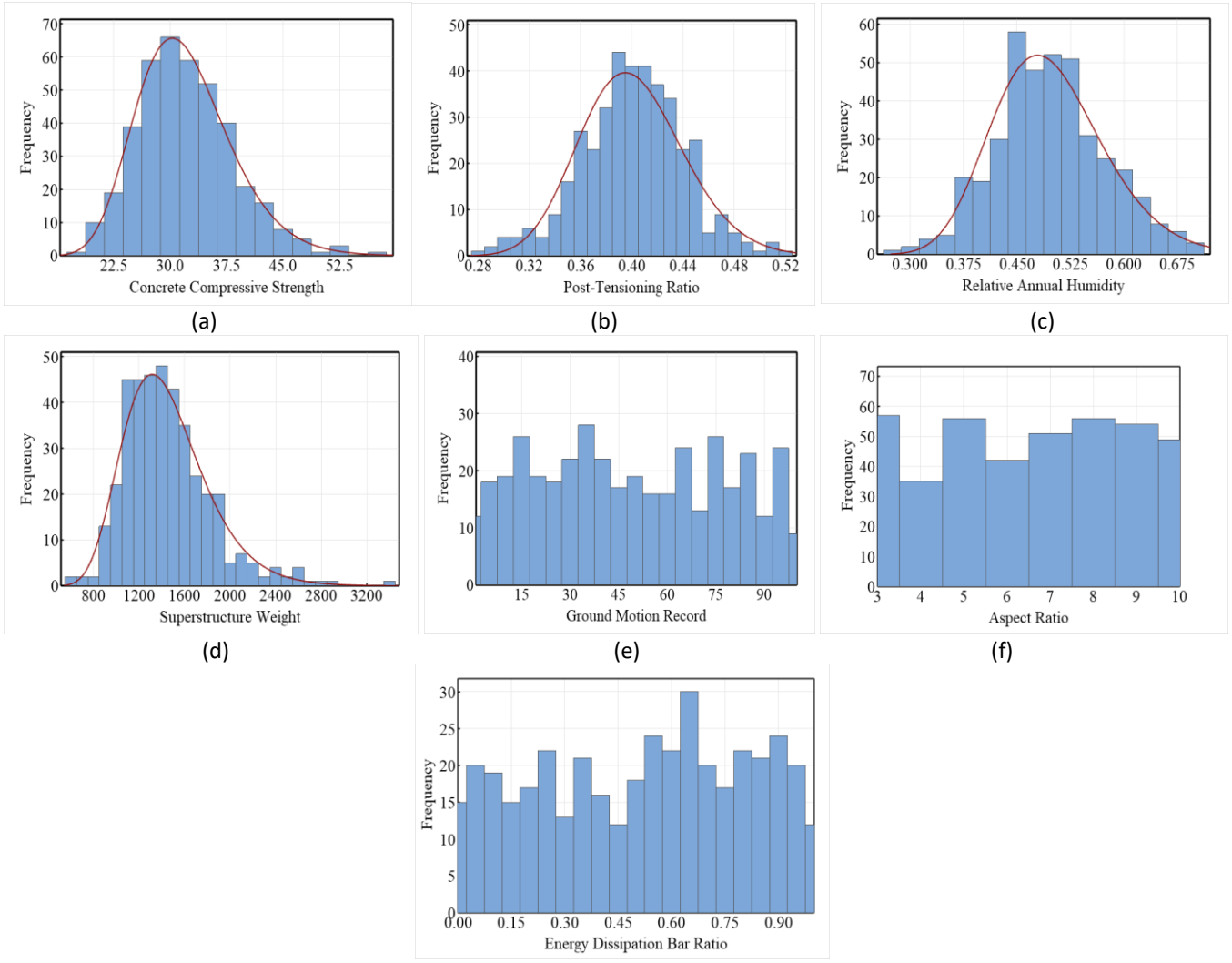

Fig. 3. Histograms of numerical features: (a) concrete compressive strength, (b) post-tensioning ratio, (c) relative annual humidity, (d) superstrucutre weight, (e) ground motion record, (f) aspect ratio, and (g) energy dissipation bar ratio.

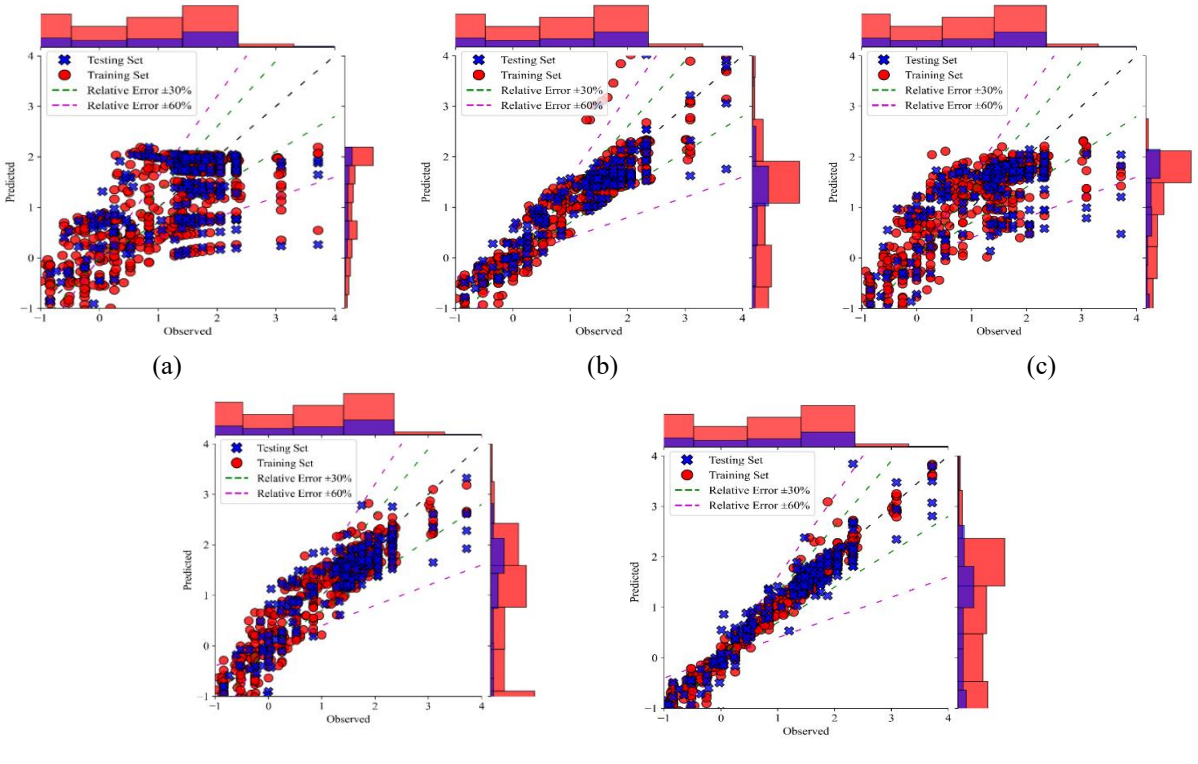

Fig. 4. Scattered plots of ML predictive models: (a) LR, (b) RF, (c) ANN, (d) KNN, and (e) XGB.

re-produces the results that it was trained with. Lines corresponding to relative errors of ±30% and ±60% are also plotted. The scatters shown in Fig. 4 are accompanied by histograms of the observed and predicted values on the plot margins, demonstrating the distribution of reliability indices of the database (observed) and the estimated models (predicted). A considerable number of scattered points in Fig. 4a have relative errors of larger than ±30% and ±60%. A similar but slightly better trend is observable in Fig. 4c for ANN predictive model. The errors for RF, KNN, and XGB are mostly smaller than ±30% and ±60% showing the capability of these algorithms in the prediction of the reliability indices of SCPT piers.

The accuracy of the predictive models is compared in Fig. 5. It is observable thar LR has the weakest predictive model among other models with $R^2 = 0.67$ and RMSE = 0.26. The predictive model of ANN is also weak with $R^2 = 0.77$ and RMSE = 0.19. KNN and RF are acceptable choices for prediction of reliability index of SCPT piers with $R^2 = 0.81$ and RMSE = 0.15 and $R^2 = 0.86$ and RMSE = 0.1, respectively. XGB with R2 = 0.9 and RMSE = 0.04 has the best performance and is able to predict the reliability index of SCPT piers with a high precision. The closeness of results between testing and training sets demonstrates that the models are not prone to overfitting.

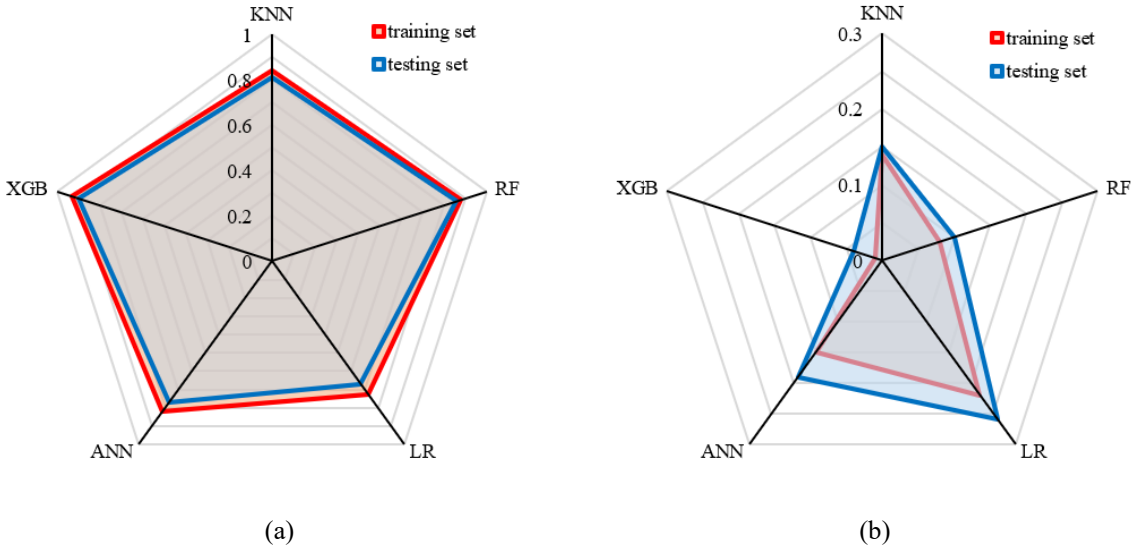

Fig. 5. Performance comparison of ML predictive models: (a) R-squared and (b) RMSE.

IV. Conclusions

In this paper, the application of ML methods on an SRA problem is investigated. The long-term reliability of SCPT piers under the influence of prestress loss is scrutinized through the MCS method. The database is created by FEM through a randomized experiment with stochastic parameters taking different design conditions into account. The database consists of 4000 input-output pairs, divided into training (80%) and testing (20%) sets. Bayesian search algorithm is utilized to optimize the hyperparameters of ML algorithms. For the comparison of the accuracy of the predictive models, R-squared and RMSE metrics are employed. The following conclusions are yield:

1) Due to the nonlinear relationship between the features and the target, the LR model shows a weak performance in predicting the reliability index of SCPT piers. Considerable number of estimations with large (> ±30% and ±60%) relative errors, and $R^2 = 0.67$ and RMSE = 0.26 suggest it.

2) The predictive model of RF (representative of tree-based algorithms) provides more accurate predictions; about 28% more accurate than the LR model, indicating the capability of tree-based models in mapping the nonlinear relationships between features and targets.

3) The deep learning-based algorithm, ANN, cannot have accurate predictions for this particular problem with $R^2 = 0.77$ and RMSE = 0.19. Yet, it is approximately 15% more accurate than LR model.

4) The comparison of the metrics used in this study exhibited that XGB model (representative of boosting algorithms) has the highest accuracy with R2 = 0.9 and RMSE = 0.04.

5) The closeness of results between testing and training sets demonstrates that the overfitting is avoided, especially in tree-based algorithms that are prone to it, showing the effectiveness of the Bayesian search technique for HPO of the ML models.

1.1.1.1.1 References

[1] A. Chen, X. Zhang and Z. Zhou, "Machine learning: Accelerating materials development for energy storage and conversion," *InfoMat,* vol. 2, no. 3, pp. 553-576, 2020.

[2] J. E. Hurtado, Structural reliability: statistical learning perspectives, Berlin Heidelberg: Springer, 2004.

[3] I. Flood, "Towards the next generation of artificial neural networks for civil engineering," *Advanced Engineering Informatics,* vol. 22, no. 1, pp. 4-14, 2008.

[4] B. Todorov and A. M. Billah, "Post-earthquake seismic capacity estimation of reinforced concrete bridge piers using Machine learning techniques," *Structures,* vol. 41, pp. 1190-1206, 2022.

[5] K. H. Turan and A. M. Yanmaz, "Reliability-based optimization of river bridges using artificial intelligence techniques," *Canadian Journal of Civil Engineering,* vol. 38, no. 10, pp. 1103-1111, 2011.

[6] J. Li, A. Li and M. Q. Feng, "Sensitivity and Reliability Analysis of a Self-Anchored Suspension Bridge," *Journal of Bridge Engineering,* vol. 18, no. 8, pp. 703-711, 2012.

[7] P. Poorahad A. and M. R. Shiravand, "Segments arrangement effect on improvement of self-centering precast post-tensioned segmental piers seismic performance," *Structural Concrete,* vol. 25, no. 1, pp. 185-206, 2024.

[8] P. Poorahad A. and M. R. Shiravand, "Seismic reliability analysis of self-centering post-tensioned piers under influence of prestress loss," *Engineering Structures,* vol. 314, no. 118315, 2024.

[9] E. Nabizadeh and A. Parghi, "Artificial neural network and machine learning models for predicting the lateral cyclic response of post-tensioned base rocking steel bridge piers," *Asian Journal of Civil Engineering,* vol. 25, no. 1, pp. 511-523, 2023.

[10] C. N. Luoung, C. Yang and M. Ezzeldin, "Genetic Programming–Based Drift Ratio Limit Models for Segmental Posttensioned Precast Concrete Piers," *Journal of Bridge Engineering,* vol. 28, no. 2, p. 04022149, 2022.

[11] F. McKenna, "OpenSees: a framework for earthquake engineering simulation," *Computing in Science & Engineering,* vol. 13, no. 4, pp. 58-66, 2011.

[12] E. Keyde, "Friction losses in prestressed steel by equivalent load method," *PCI Journal,* vol. 35, no. 2, pp. 74-77, 1990.

[13] A. E. Naaman and S. Chao, Prestressed concrete analysis and design: Fundamentals, 1982.

[14] H. M. Dawood and M. ElGawady, "Performance-based seismic design of unbonded precast post-tensioned concrete filled GFRP tube piers," *Composites Part B: Engineeing,* vol. 44, no. 1, pp. 357-367, 2013.

[15] Y. Itoh, M. Wada and C. Liu, "Lifecycle environmental impact and cost analyses of steel bridge piers with seismic risk," in *The 9th international conference on structural safety and reliability*.

[16] S. Saraygord Afshari, F. Enayatollahi, X. Xu and X. Liang, "Machine learning-based methods in structural reliability analysis: A re," *Reliability Engineering and System Safety,* vol. 219, no. 108223, 2022.

[17] A. T. Council, Quantification of building seismic performance factors, Washington, DC: US Department of Homeland Security, FEMA, 2009.

[18] A. S. o. C. Engineers, Minimum design loads and associated criteria for buildings and other structures, Reston, Virginia: American Society of Civil Engineers, 2016.

[1] A. Chen, X. Zhang and Z. Zhou, "Machine learning: Accelerating materials development for energy storage and conversion," InfoMat, vol. 2, no. 3, pp. 553-576, 2020.

[2] J. E. Hurtado, Structural reliability: statistical learning perspectives, Berlin Heidelberg: Springer, 2004.

[3] I. Flood, "Towards the next generation of artificial neural networks for civil engineering," Advanced Engineering Informatics, vol. 22, no. 1, pp. 4-14, 2008.

[4] B. Todorov and A. M. Billah, "Post-earthquake seismic capacity estimation of reinforced concrete bridge piers using Machine learning techniques," Structures, vol. 41, pp. 1190-1206, 2022.

[5] K. H. Turan and A. M. Yanmaz, "Reliability-based optimization of river bridges using artificial intelligence techniques," Canadian Journal of Civil Engineering, vol. 38, no. 10, pp. 1103-1111, 2011.

[6] J. Li, A. Li and M. Q. Feng, "Sensitivity and Reliability Analysis of a Self-Anchored Suspension Bridge," Journal of Bridge Engineering, vol. 18, no. 8, pp. 703-711, 2012.

[7] P. Poorahad A. and M. R. Shiravand, "Segments arrangement effect on improvement of self-centering precast post-tensioned segmental piers seismic performance," Structural Concrete, vol. 25, no. 1, pp. 185-206, 2024.

[8] P. Poorahad A. and M. R. Shiravand, "Seismic reliability analysis of self-centering post-tensioned piers under influence of prestress loss," Engineering Structures, vol. 314, no. 118315, 2024.

[9] E. Nabizadeh and A. Parghi, "Artificial neural network and machine learning models for predicting the lateral cyclic response of post-tensioned base rocking steel bridge piers," Asian Journal of Civil Engineering, vol. 25, no. 1, pp. 511-523, 2023.

[10] C. N. Luoung, C. Yang and M. Ezzeldin, "Genetic Programming–Based Drift Ratio Limit Models for Segmental Posttensioned Precast Concrete Piers," Journal of Bridge Engineering, vol. 28, no. 2, p. 04022149, 2022.

[11] F. McKenna, "OpenSees: a framework for earthquake engineering simulation," Computing in Science & Engineering, vol. 13, no. 4, pp. 58-66, 2011.

[12] E. Keyde, "Friction losses in prestressed steel by equivalent load method," PCI Journal, vol. 35, no. 2, pp. 74-77, 1990.

[13] A. E. Naaman and S. Chao, Prestressed concrete analysis and design: Fundamentals, 1982.

[14] H. M. Dawood and M. ElGawady, "Performance-based seismic design of unbonded precast post-tensioned concrete filled GFRP tube piers," Composites Part B: Engineeing, vol. 44, no. 1, pp. 357-367, 2013.

[15] Y. Itoh, M. Wada and C. Liu, "Lifecycle environmental impact and cost analyses of steel bridge piers with seismic risk," in The 9th international conference on structural safety and reliability.

[16] S. Saraygord Afshari, F. Enayatollahi, X. Xu and X. Liang, "Machine learning-based methods in structural reliability analysis: A re," Reliability Engineering and System Safety, vol. 219, no. 108223, 2022.

[17] A. T. Council, Quantification of building seismic performance factors, Washington, DC: US Department of Homeland Security, FEMA, 2009.

[18] A. S. o. C. Engineers, Minimum design loads and associated criteria for buildings and other structures, Reston, Virginia: American Society of Civil Engineers, 2016.

1) Pooria Poorahad A.: Ph.D. candidate in Earthquake Engineering, Faculty of Civil, Water, and Environmental Engineering, Shahid Beheshti University
ORCID ID: 0000-0002-7173-9975
Email: p_poorahadanzabi@sbu.ac.ir
2) Mahmoud R. Shiravand: Associate Professor, Faculty of Civil, Water, and Environmental Engineering, Shahid Beheshti University
ORCID ID: 0000-0002-8740-2242
Email: m_shiravand@sbu.ac.ir
3) Mahtab Ebadati: B.Sc. in Civil Engineering, Faculty of Civil, Water, and Environmental Engineering, Shahid Beheshti University
Email: m.ebadati@mail.sbu.ac.ir